



**HAL**  
open science

## Detection of Spin Reversal via Kondo Correlation in Hybrid Carbon Nanotube Quantum Dots

Subhadeep Datta, Ireneusz Weymann, Anna Plomińska, Emmanuel Flahaut, Lætitia Marty, Wolfgang Wernsdorfer

► **To cite this version:**

Subhadeep Datta, Ireneusz Weymann, Anna Plomińska, Emmanuel Flahaut, Lætitia Marty, et al.. Detection of Spin Reversal via Kondo Correlation in Hybrid Carbon Nanotube Quantum Dots. ACS Nano, 2019, 13 (9), pp.10029-10035. 10.1021/acsnano.9b02091 . hal-02317479

**HAL Id: hal-02317479**

**<https://hal.science/hal-02317479>**

Submitted on 16 Oct 2019

**HAL** is a multi-disciplinary open access archive for the deposit and dissemination of scientific research documents, whether they are published or not. The documents may come from teaching and research institutions in France or abroad, or from public or private research centers.

L'archive ouverte pluridisciplinaire **HAL**, est destinée au dépôt et à la diffusion de documents scientifiques de niveau recherche, publiés ou non, émanant des établissements d'enseignement et de recherche français ou étrangers, des laboratoires publics ou privés.




## Open Archive Toulouse Archive Ouverte (OATAO)

OATAO is an open access repository that collects the work of Toulouse researchers and makes it freely available over the web where possible

This is an author's version published in: <http://oatao.univ-toulouse.fr/24384>

**Official URL:** <https://doi.org/10.1021/acsnano.9b02091>

**To cite this version:**

Datta, Subhadeep and Weymann, Ireneusz and Płomińska, Anna and Flahaut, Emmanuel  and Marty, Lætitia and Wernsdorfer, Wolfgang *Detection of Spin Reversal via Kondo Correlation in Hybrid Carbon Nanotube Quantum Dots.* (2019) ACS Nano, 13 (9). 10029-10035. ISSN 1936-0851

Any correspondence concerning this service should be sent to the repository administrator: [tech-oatao@listes-diff.inp-toulouse.fr](mailto:tech-oatao@listes-diff.inp-toulouse.fr)

# Detection of Spin Reversal *via* Kondo Correlation in Hybrid Carbon Nanotube Quantum Dots

Subhadeep Datta,<sup>\*,†,‡,§</sup> Ireneusz Weymann,<sup>¶</sup> Anna Płomińska,<sup>¶</sup> Emmanuel Flahaut,<sup>§</sup> L  titia Marty,<sup>‡</sup> and Wolfgang Wernsdorfer<sup>‡,||</sup>

<sup>†</sup>School of Physical Sciences, Indian Association for the Cultivation of Science, 2A & B Raja S. C. Mullick Road, Jadavpur, Kolkata 700032, India

<sup>‡</sup>Institut N  el, CNRS & Universit   Joseph Fourier, BP 166, F 38042 Grenoble Cedex 9, France

<sup>¶</sup>Faculty of Physics, Adam Mickiewicz University, ul. Uniwersytetu Poznańskiego 2, 61 614 Poznań, Poland

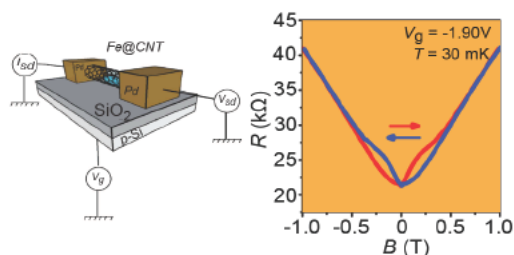
<sup>§</sup>CIRIMAT, Universit   de Toulouse, CNRS, INPT, UPS, UMR CNRS UPS INP No 5085, Universit   Toulouse 3 Paul Sabatier, B  t. CIRIMAT, 118, Route de Narbonne, 31062 Toulouse Cedex 9, France

<sup>||</sup>Physikalisches Institut and Institute of Nanotechnology, Karlsruhe Institute of Technology, Wolfgang Gaede Strasse 1, 76131 Karlsruhe, Germany

## Supporting Information

**ABSTRACT:** We experimentally investigate the electronic transport through a double wall carbon nanotube filled with Fe nanoparticles. At very low temperatures, the Kondo effect is observed between the confined electrons in the nanotube quantum dot and the delocalized electrons in the leads connecting the nanotube. We demonstrate that the presence of magnetic nanoparticles in the inner core of the nanotube results in a hysteretic behavior of the differential resistance of the system when the magnetic field is varied. This behavior is observed in the Kondo diamonds of the stability diagram, and the magnitude of hysteresis varies with the strength of the Kondo correlations in different diamonds. Our findings are corroborated with accurate numerical renormalization group calculations performed for an effective low energy model involving fluctuations of the spin on the orbital level of the nanotube due to spin flips of the nanoparticles.

**KEYWORDS:** Kondo effect, magnetic nanoparticles, magnetization reversal, magnetotransport, molecular electronics, quantum dots, carbon nanotube



Nanostructured quantum dots (QDs) are ideal model systems to probe many body electronic correlations, such as the ones leading to the Kondo effect. In this effect, an entangled state is formed as a result of screening of the localized spin in the dot by surrounding conduction electrons,<sup>1–4</sup> analogous to the Kondo problem in bulk metals containing magnetic impurities.<sup>5</sup> The presence of a zero bias conductance peak below a certain characteristic temperature (the Kondo temperature,  $T_K$ ) is the hallmark of the formation of a Kondo cloud in the quantum dots coupled by tunnel barriers to source–drain electrodes.<sup>6</sup> This effect can be used as a spin sensitive probe to detect the interaction of a local spin in the host QD with large spin of magnetic adatoms or molecules in an electric field controlled way. The competition between the exchange interaction of magnetic moments and the Kondo cloud in the QD has been well studied in different quantum dot systems involving direct interaction between spins in a

double quantum dot,<sup>7,8</sup> the exchange interaction with ferromagnetic leads,<sup>9,10</sup> and the indirect Ruderman–Kittel–Kasuya–Yoshida (RKKY) interaction of two QDs separated by a larger dot.<sup>11</sup> A recent study on the Kondo effect in a Au nanowire with magnetic impurities such as Co shows that the zero bias Kondo peak splits due to the RKKY interaction between the net spin of the quantum dot and magnetic impurities.<sup>12</sup> To our knowledge, the research so far has been mainly focused on the interplay of the Kondo effect in QDs and the local magnetic field from guest atoms. However, the effect of magnetization reversal of magnetic moments on the electron transport of Kondo correlated QDs, as demonstrated by hysteresis in conductance of QDs in the Coulomb blockade

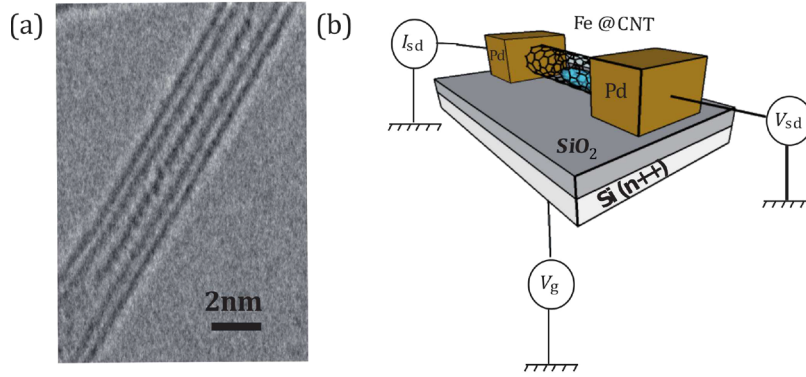


Figure 1. (a) TEM image of a double wall nanotube filled with iron particles. Particles form small dots (1–1.5 nm) inside the inner wall. (b) Schematic representation of the three terminal nanotube device. Pd contacts are designed on top of a SiO<sub>2</sub>/Si (n++) wafer used as a back gate.

regime, is still unexplored. Understanding the dynamical properties of the hybrid QD system stemming from the magnetic anisotropy of adatoms in the context of many body physics could be very useful for future applications in information storage and magnetic logic. To choose a suitable QD system for this, we have found that carbon nanotube based (CNT) dots are advantageous relative to the other dots due to (i) higher Kondo temperature and (ii) large Landè  $g$  factor.<sup>13,14</sup> In addition, nanotubes possess a unique ability to encapsulate foreign materials inside their inner cores, which can protect the molecules from environmental influences. Taking this into account, a nanotube QD in the Kondo regime, filled with magnetic nanoparticles, can be a good model system to study the effect of the spin flip of magnetic nanoparticles on the Kondo assisted magnetotransport.

In this article, we report on the low temperature (from 30 mK to 1 K) electrical transport measurements of a double wall carbon nanotube (DWCNT) filled with Fe nanoparticles. The measurements of electrical conductance through the system revealed the existence of the Kondo effect, which has been studied thoroughly with respect to temperature ( $T$ ) and external magnetic field ( $B$ ). Hysteresis in differential resistance ( $R$ ) as a function of magnetic field ( $B$ ) is observed only in the Kondo (odd electron number) diamonds of the nanotube. The dependence of the hysteresis on the temperature and magnetic field attests the influence of magnetization reversal of magnetic nanoparticles. The experimental observations are corroborated quite well with numerical renormalization group calculations for an effective low energy model considering the presence of magnetic nanoparticles causing fluctuation of the spin on the orbital level of the nanotube.

We note that the Kondo effect in carbon nanotube quantum dots has already been a subject of extensive theoretical and experimental studies.<sup>13–15</sup> Moreover, the properties of CNTs with encapsulated impurities have also been analyzed.<sup>16–19</sup> However, none of these works have reported the hysteretic behavior of magnetoresistance associated with spin reversal of magnetic nanoparticles.

We use double wall carbon nanotubes filled with Fe nanoparticles to fabricate quantum dots connected between two metallic electrodes (see Methods for details).<sup>20,21</sup> SQUID measurements and Mossbauer spectroscopy are performed to confirm the existence of magnetic nanoparticles in the hybrid.<sup>22</sup> In addition, transmission electron microscopy (TEM) revealed partial filling of the hybrid double wall CNTs [Figure 1(a)]. Nanotube junctions that are 300–400

nm wide were fabricated by electron beam lithography (EBL), followed by metal evaporation (50 nm of Pd). The scheme of the device is shown in Figure 1(b). The electron transport measurements were performed in a dilution refrigerator with a base temperature of 30 mK.

Figure 2(a) shows a plot of the linear response differential conductance ( $G$ ) versus the gate voltage. Regular Coulomb

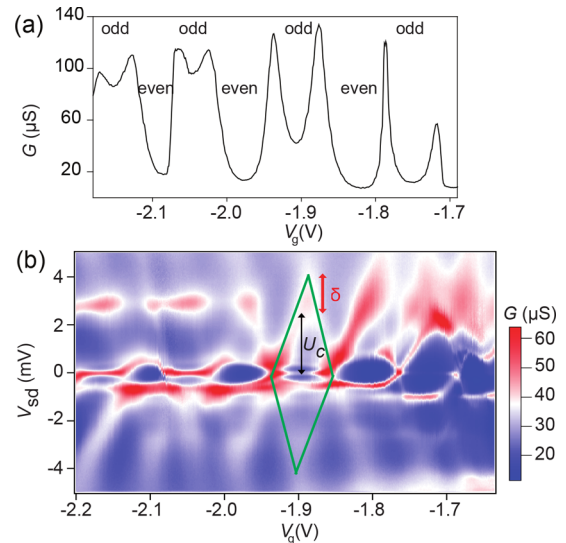


Figure 2. (a) Differential conductance  $G$  for a zero bias gate sweep from  $V_g = -2.2$  V to  $-1.65$  V. The Coulomb peaks are separated by low and high conductance regions. Odd nanotube occupancy is deduced from intermediate differential conductance Kondo ridges. (b) Bias spectroscopy map at  $T = 30$  mK. A typical alternating pattern of even and odd occupation diamonds is observed with characteristic Kondo ridges at zero bias. The different capacitances with electrodes are calculated from the slope of the diamond constituted by the green lines. The charging energy  $U_C$  and the level spacing  $\delta$  have been marked by black and red arrows, respectively.

oscillations are visible with alternating strong and weak blocked conductance between the peaks. This feature is visible on the complete Coulomb diagram as blocked diamonds corresponding to even occupancy of the quantum dot, followed by odd diamonds exhibiting zero bias high conductance ridges [Figure 2(b)]. The measured stability diagram is typical of the Kondo effect in a QD with good coupling to the contacts.<sup>23</sup> From these Coulomb diamonds, we



extracted the charging energy  $U_C \approx 2.6$  meV and the spacing between the spin degenerate levels  $\delta \approx 1.5$  meV. The device total capacitance  $C = C_s + C_d + C_g = 61$  aF was deduced from the charging energy. The slopes [as indicated in Figure 2(b)] of the diamond sides ( $\alpha_s = 0.08$  and  $\alpha_d = 0.12$ ) provide the different capacitances:  $C_s = 24$  aF,  $C_d = 34$  aF, and  $C_g = 3$  aF. The distance between the peaks in Figure 2(a)  $\Delta V_g \approx 80$  mV is scaled by the coupling to the gate,  $\alpha = \frac{U_C + \delta}{e\Delta V_g} = 0.04$ , comparable to what we have calculated from the ratio of the gate capacitance to the total capacitance,  $\frac{C_g}{C} = 0.05$ .

## RESULTS AND DISCUSSION

The influence of an external magnetic field ( $B$ ) on the electrical properties of the device is shown in Figure 3. The

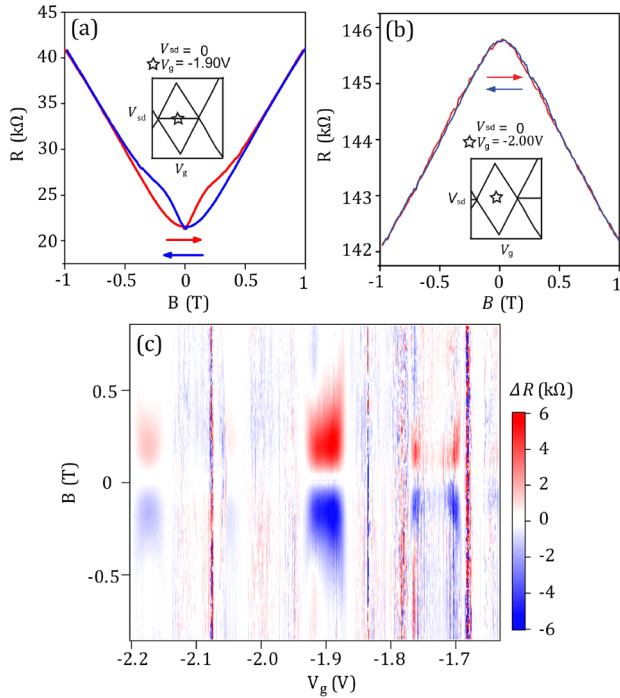


**Figure 3.** (a, b) Differential magnetoresistance (back and forth) measured in the middle of odd (a) and even (b) occupation diamonds. (a) At  $V_g = -1.90$  V (odd case) the differential resistance shows hysteresis around zero magnetic field. (b) No hysteresis is observed for  $V_g = -2.00$  V (even case). (c) Color plot of resistance hysteresis  $\Delta R$  as a function of the gate voltage  $V_g$ . The red, blue, and white colors correspond to positive, negative, and zero hysteresis, respectively.

magnetic field is swept from  $-1$  T to  $+1$  T (trace) at a constant rate ( $0.03$  T  $s^{-1}$ ) and return (retrace) (also see Figure S5). Figure 3(a,b) show the linear response differential resistance  $R$  as a function of the magnetic field  $B$  (trace and retrace) inside the even diamond [Figure 3(b)] and on the Kondo ridge [Figure 3(a)]. The magnetoresistance is negative and without hysteresis for the even occupation case. On the contrary, positive magnetoresistance ( $45$  k $\Omega$ /T) is observed along with hysteresis for the odd occupation case. The hysteresis is symmetric with respect to zero magnetic field and exhibits pronounced jumps from  $B = \pm 0.05$  T to  $B = \pm 0.45$  T [see Figure 3(b)]. These features are not observed in similar devices made with empty DWNTs (Figures S3 and S4) and are

thus attributed to the enclosed particles' spin reversal at their switching field,  $B_{sw}$ .<sup>24</sup> We note that a similar hysteresis in electrical transport induced by the switching of magnetization of a nonmagnetic QD has been predicted in different hybrid QD devices.<sup>25–27</sup> However, in our case it is strongly related to the Kondo effect in a CNT, which will be discussed below. Note that all measurements presented in the article have been performed on one sample out of four samples that shows hysteresis in Kondo ridges of a filled carbon nanotube. The results are qualitatively similar in the other three devices.

To quantify the magnitude of the hysteresis of resistance, we introduce  $\Delta R$ , defined as the difference between the trace and retrace magnetoresistance curves,  $\Delta R = R_{trace} - R_{retrace}$ , and plotted as a color map in Figure 3(c). By comparing the hysteresis map [Figure 3(c)] and the stability diagram [Figure 2(b)], one can easily notice that hysteresis is present only in the Kondo diamonds. Moreover, the hysteresis magnitude ( $|\Delta R|$ ) is strongly dependent on the value of conductance in the Kondo ridges. For example,  $|\Delta R_{max}| = 6$  k $\Omega$  is observed at  $V_g = -1.90$  V, where  $G(V_{sd} = 0) = 20$   $\mu S$ , whereas larger conductance  $G(V_{sd} = 0) = 50$   $\mu S$  at  $V_g = -2.18$  V results in a weaker hysteresis with  $|\Delta R_{max}| = 2$  k $\Omega$ . Larger conductance at a Kondo ridge is associated with a higher Kondo temperature. Since the Kondo temperature strongly depends on the ratio of  $\Gamma/U_C$ , where  $\Gamma$  is the energy level broadening and  $U_C$  is the charging energy, and increases when this ratio becomes larger,<sup>3</sup> higher  $T_K$  corresponds to stronger correlations<sup>6</sup> for the considered gate voltage. As the magnetic hysteresis is a rather small effect ( $|\Delta R_{B_{0to0.45T}}| < |\Delta R_{B_{-1Tto0T}}|$ ) compared to large magnetoresistance behavior in the Kondo ridge, depending upon the Kondo correlations, hysteresis strongly varies in different Kondo ridges (Figure S1).<sup>28</sup> Figure S2 shows the hysteresis of the resistance as a function of the magnetic field in the plane of the carbon nanotube. The magnetic field at which hysteresis vanishes changes significantly as a function of field direction.<sup>38,39</sup> However, the result does not really follow the well known Stoner–Wohlfarth model, which describes the magnetization reversal of one single nanoparticle by uniform rotation of the magnetization.<sup>24,38</sup> The presence of many nanoparticles inside the nanotube having different preferential magnetization orientation with respect to the host carbon nanotube axis could be responsible for this feature.

In Figure 4(a), we present the temperature dependence of the zero bias Kondo peak measured at  $V_g = -1.91$  V. The estimation of the Kondo temperature extracted from the half width at half maximum of the zero bias peak ( $\frac{1}{2}fwhm = \frac{e\Delta V_{sd}}{k_B} \approx 750$  mK) is quite comparable to the one obtained from the conductance profile at different temperatures shown in Figure 4(a) ( $T_K \approx 500$  mK).<sup>3</sup> Figure 4(b) shows that the magnitude of hysteresis decreases as the temperature goes up from  $T = 30$  mK to  $T = 400$  mK and completely disappears for  $T > 400$  mK. At  $T = 400$  mK, the magnitude of the Kondo peak is around 50% lower compared to its low temperature value ( $T \approx 40$  mK). This is a direct consequence of the fact that the Kondo correlations vanish for temperatures beyond the Kondo temperature ( $T > T_K$ ) due to thermal fluctuations. Consequently, the device resistance recovers then a nonhysteretic behavior. Similarly, as shown in Figure 4(c), the hysteresis is also completely washed out for  $V_{sd} \gtrsim 300$   $\mu V$ . Comparing with Figure 4(a), this corresponds to the tail of the Kondo profile. The conductance drops then by 80% from its peak value at  $V_{sd} = 0$ .

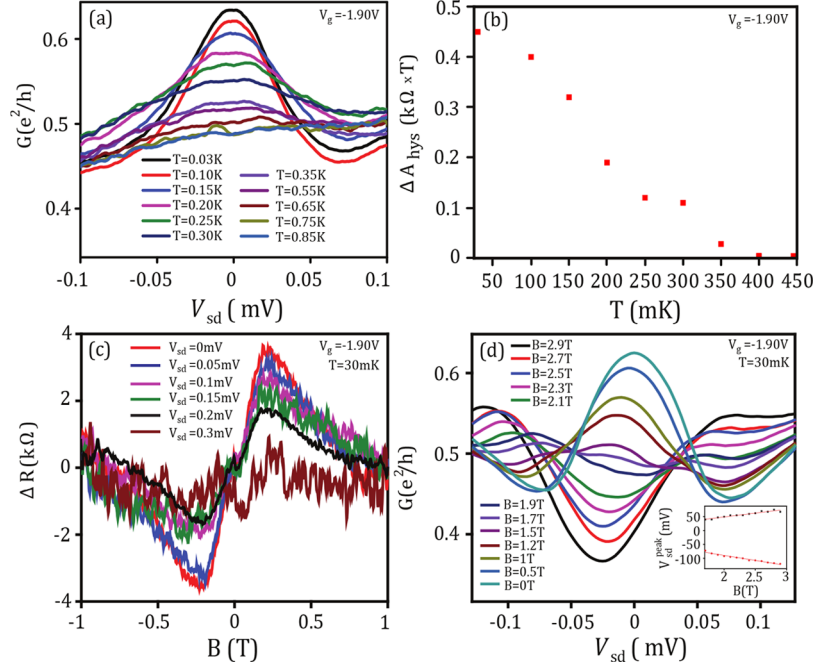


Figure 4. (a) Temperature dependence of the Kondo peak. The height of the peak at zero bias decreases as the temperature increases. The measured Kondo temperature is  $T_K \approx 500$  mK. On the other hand, the Kondo temperature extracted from the half width at half maximum of zero bias peak in  $G$  is  $T_K \approx 750$  mK. (b) Temperature dependence of the area of the hysteresis loop. The hysteresis disappears around  $T_B \approx 400$  mK. (c) Hysteresis for different bias voltages. It becomes washed out for  $V_{sd} \gtrsim 300$   $\mu$ V. (d) Bias voltage dependence of the conductance for different magnetic fields. Inset presents the dependence of the position of the split Kondo peak ( $V_{sd}^{\text{peak}}$ ) on magnetic field  $B$ .

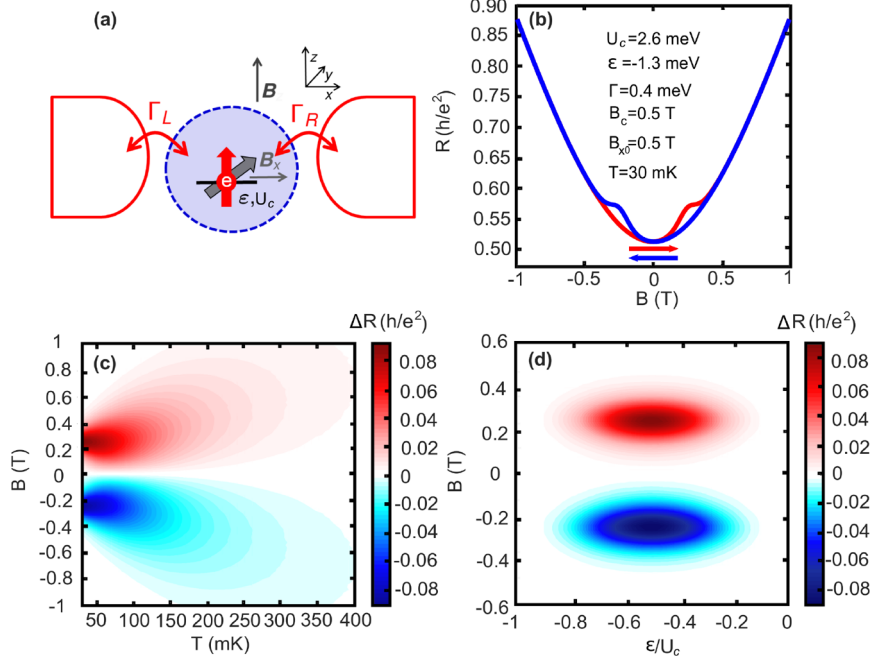


Figure 5. (a) Cartoon of the theoretical model used. Single orbital level of energy  $\epsilon$  and Coulomb correlations  $U_C$  is tunnel coupled to the leads with respective strengths  $\Gamma_L$  and  $\Gamma_R$ . There is an external magnetic field  $B$  applied to the system. It is assumed that the presence of nanoparticles inside the inner tube results in an additional  $x$  component of magnetic field. (b) Magnetic field dependence of the linear resistance  $R = 1/G$  with characteristic hysteretic behavior. The parameters of the system are  $U_C = 2.6$  meV,  $\epsilon = -1.3$  meV,  $\Gamma = 0.4$  meV,  $B_c = 0.5$  T,  $B_{x0} = 0.5$  T, and  $T = 30$  mK. The red curve corresponds to the forward sweep of  $B$ , while the blue curve is for the opposite sweep, for which the coercive field of nanoparticles  $B_c$  flips sign. The map of resistance change  $\Delta R$  as a function of magnetic field  $B$  and (c) temperature  $T$  and (d) orbital level position  $\epsilon$  shows that the hysteretic behavior vanishes with increasing  $T$  or detuning the system from an odd electron occupation regime.

Figure 4(d) shows the Kondo peak splitting with an applied magnetic field.<sup>28–31</sup> The typical linear evolution of the splitting

of the two Kondo components is observed. From the position of the two peaks ( $V_{sd}^{\text{peak}}$ ) it is possible to extract the  $g$  factor

using the formula  $\pm \frac{1}{2} g \mu_B B = e V_{sd}^{\text{peak}}$ . The  $g$  factor comes out to be  $g \approx 1.97$  and  $g \approx 2.42$  for the positive and negative bias voltage peak, respectively, which agrees reasonably well with previous investigations on carbon nanotubes.<sup>32,33</sup> From the intercepts of the linear fits, the minimum magnetic field to split the Kondo peak,  $B_K \approx 340$  mT, is found, which is large compared to the field change associated with the hysteresis  $\Delta B \approx 200$  mT [see Figure 3(a)], and corresponds to the Kondo temperature  $T_K \approx 430$  mK, since  $g \mu_B B_K = k_B T_K$  for a spin  $\frac{1}{2}$  Kondo effect.<sup>34</sup>

## THEORETICAL ANALYSIS

**Model and Method.** To model the system in the Kondo regime, we propose an effective low energy model, which is schematically shown in Figure 5(a). We consider one orbital level of energy  $\varepsilon$  and Coulomb correlations  $U_C$ , which is tunnel coupled to external leads, with coupling strengths,  $\Gamma_L$  and  $\Gamma_R$ , for the left and right lead, respectively. We assume that the presence of magnetic nanoparticles causes the spin on the orbital level to rotate, as if an additional  $x$  component of magnetic field was present in the system. We thus have the following effective Hamiltonian of the system,  $H = H_{\text{el}} + H_{\text{imp}} + H_{\text{tun}}$ . The first term describes the noninteracting electrons in the leads:

$$H_{\text{el}} = \sum_{rk\sigma} \varepsilon_{rk} c_{rk\sigma}^\dagger c_{rk\sigma} \quad (1)$$

where  $c_{rk\sigma}^\dagger$  is the creation operator of an electron with spin  $\sigma$ , momentum  $k$ , and energy  $\varepsilon_{rk}$  in the lead  $r$ . The second term of the Hamiltonian models the complex impurity and has the following form:

$$H_{\text{imp}} = \sum_{\sigma} \varepsilon n_{\sigma} + U_C n_{\uparrow} n_{\downarrow} + B s_z + B_x s_x \quad (2)$$

Here,  $n_{\sigma} = d_{\sigma}^\dagger d_{\sigma}$ , where  $d_{\sigma}^\dagger$  creates a spin  $\sigma$  electron in the orbital level of energy  $\varepsilon$ . The spin operator of electrons on the orbital level is described by  $\vec{s} = (1/2) \sum_{\sigma, \sigma'} d_{\sigma}^\dagger \vec{\sigma}_{\sigma\sigma'} d_{\sigma'}$ , with  $\vec{\sigma}$  being the vector of Pauli spin matrices, while  $B$  and  $B_x$  denote the  $z$ th and  $x$ th components of the magnetic field in energy units ( $g \mu_B \equiv 1$ ).

Finally, the last term of the Hamiltonian accounts for tunneling processes between the orbital level and external leads:

$$H_{\text{tun}} = \sum_{rk\sigma} V_r (c_{rk\sigma}^\dagger d_{\sigma} + d_{\sigma}^\dagger c_{rk\sigma}) \quad (3)$$

where  $V_r$  denotes the corresponding tunnel matrix elements. The total coupling between the leads and the orbital level is given by  $\Gamma = \Gamma_L + \Gamma_R$ , where  $\Gamma_r = \pi \rho_r V_r^2$  and  $\rho_r$  is the density of states of lead  $r$ , which is assumed to be flat.

In our effective model, the presence of magnetic nanoparticles is assumed to cause a rotation of the spin in the orbital level. This happens when the external magnetic field  $B$  is on the order of the coercive field of nanoparticles  $B_c$ . We associate the magnitude of additional magnetic field component  $B_x$  acting on electrons residing in the orbital level with the fluctuations of magnetizations of nanoparticles. Consequently, we assume  $B_x = B_{x0} \text{sech}[(B - B_c/2)/2T]$ , where  $B_{x0}$  is the maximum value of the field. Suppose we start the magnetic field sweep from negative to positive values. Then, the magnetization of nanoparticles flips its orientation

when magnetic field  $B$  is on the order of  $B_c$ . On the other hand, for the backward sweep, the magnetization of nanoparticles is reversed back when  $B \sim -B_c$ . Consequently, in our effective model we assume that the  $x$  component of magnetic field  $B_x$ , which is directly associated with magnetization reversal of nanoparticles, becomes enhanced either for  $B = B_c/2$  or for  $B = -B_c/2$ , depending on the sweep direction.

In order to study the transport properties in the Kondo regime, we use the density matrix numerical renormalization group (NRG) method.<sup>36,37</sup> In the NRG, the electrodes' conduction band is mapped into the semi infinite chain with exponentially decreasing hoppings, which can be solved in an iterative way. By using NRG, we accurately determine the orbital level spectral function  $A(\omega) = \sum_{\sigma} A_{\sigma}(\omega)$ , where  $A_{\sigma}(\omega) = -\frac{1}{\pi} \text{Im} \langle \langle d_{\sigma} | d_{\sigma}^{\dagger} \rangle \rangle_{\omega}$  and  $\langle \langle d_{\sigma} | d_{\sigma}^{\dagger} \rangle \rangle_{\omega}$  is the Fourier transform of the retarded Green's function  $\langle \langle d_{\sigma} | d_{\sigma}^{\dagger} \rangle \rangle_t = -i \theta(t) \langle \{ d_{\sigma}(t), d_{\sigma}^{\dagger}(0) \} \rangle$ . The spectral function allows us then to calculate the linear response conductance from the following formula:<sup>35</sup>

$$G = \frac{2e^2}{h} \frac{4\Gamma_L \Gamma_R}{\Gamma_L + \Gamma_R} \int d\omega \left( -\frac{\partial f(\omega)}{\partial \omega} \right) \pi A(\omega) \quad (4)$$

where  $f(\omega)$  is the Fermi-Dirac distribution function.

We would like to notice that, given the complexity of the real system studied, we do not intend to quantitatively fully reproduce the experimentally measured conductance curves, but rather focus on obtaining similar qualitative behavior. Therefore, in calculations we assume equal couplings to the left and right contacts,  $\Gamma_L = \Gamma_R = \Gamma/2$ ,  $U_C = 2.6$  meV, and equal  $g$  factor for the whole system  $g = 2$  and tune the other parameters to observe the desired behavior. As far as the NRG parameters are concerned, we use the discretization parameter  $\Lambda = 2$  and keep at least  $N_K = 1024$  states at each step of iterative diagonalization.

**Numerical Results.** To fit to the experimentally observed hysteretic magnetic field dependence of the resistance, we estimate  $\Gamma = 0.4$  meV and  $B_c = B_{x0} = 0.5$  T, which is on the order of experimental parameters. The calculated dependence of the linear resistance  $R = 1/G$  on  $B$  is shown in Figure 5(b), and it clearly reveals the hysteresis observed experimentally and presented in Figure 3(a). On the other hand, the dependence of  $\Delta R$  on the magnetic field and temperature reveals the suppression of hysteresis with increasing the temperature; see Figure 5(c). The temperature  $T \approx 400$  mK, at which hysteresis becomes washed out, is comparable to the temperature estimated from the experimental data. The observed hysteretic behavior also becomes suppressed when moving out of the Kondo regime, which is visible in Figure 5(d), presenting the dependence of  $\Delta R$  on  $B$  and orbital level position  $\varepsilon$ . We would like to emphasize that although the proposed theoretical model is relatively simple, it captures the experimentally observed behavior quite well. We also note that one could think of other mechanisms resulting in hysteretic dependence of  $R$  on  $B$  in the Kondo regime. In particular, the presence of magnetic nanoparticles could be modeled by exchange coupling the orbital level to an additional spin or several spins, subject to an effective magnetic field coming from neighboring magnetic nanoparticles. In this case a hysteresis in magnetic field can also be observed, but our calculations revealed (not shown) that the change in resistance is almost 2 orders of magnitude smaller than the one observed experimentally.



## CONCLUSIONS

In conclusion, we have measured the conductance through a DWCNT filled with magnetic particles in the Kondo regime. The characterization of the Kondo ridge with the temperature and magnetic field showed the existence of a typical spin  $\frac{1}{2}$  Kondo effect in our system. A magnetoresistance study of the device revealed the presence of hysteresis due to the magnetization reversal of different magnetic nanoparticles. This hysteretic behavior was observed in the odd occupation Coulomb diamonds, in which the Kondo effect develops, and was absent in the even occupation diamonds. To understand experimental findings, we proposed an effective low energy model, in which an orbital level, tunnel coupled to the leads, is subject to spin reversal at magnetic fields on the order of the coercive field of nanoparticles. The results obtained using a density matrix numerical renormalization group method corroborated the experimental data relatively well.

Our investigations demonstrate an indirect detection of the magnetization reversal of the nanoparticles through the electrical transport study of nanotube QDs in the Kondo regime. The Kondo effect enabled us to probe the magnetic activity caused by magnetic particles inside the nanotube. Indeed, filling the nanotube with well crystallized magnetic nanoparticles having large anisotropy can lead to a better understanding of the underlying physics of the interaction between Kondo spin and ferromagnetism. Our results also hint at the possibility of using CNTs as detectors of magnetization of individual magnetic objects coupled to them.

## METHODS

The DWCNTs with a number of walls selectivity of 80% were synthesized by catalytic chemical vapor deposition (CCVD). The DWNT powder was mixed with anhydrous iron(II) iodide in an approximate 1:1.3 molar ratio and subsequently annealed at 690 °C for 5 h to let melted FeI<sub>2</sub> enter the DWNT due to capillary forces. Iron islands inside the nanotubes were obtained by reducing FeI<sub>2</sub>@DWCNT in hydrogen at 250 °C for 5 h, as confirmed by SQUID measurements and Mossbauer spectroscopy. TEM revealed partial filling of the hybrid double wall CNTs. The CNTs were then dispersed on a 500 nm SiO<sub>2</sub> capped degenerately doped Si wafer used as a back gate. CNTs were localized by atomic force microscopy (AFM) using prepatterned gold electrodes as a reference system. Nanotube junctions 300–400 nm in width were fabricated by aligned EBL, followed by metal evaporation (50 nm of Pd). The electron transport measurements were performed in a dilution refrigerator with a base temperature of 30 mK.

## ASSOCIATED CONTENT

### Supporting Information

The following files are available free of charge. The Supporting Information is available free of charge on the [ACS Publications website](https://doi.org/10.1021/acsnano.9b02091) at DOI: 10.1021/acsnano.9b02091.

Magnetotransport data for a device with an empty nanotube for which the Kondo effect was observed (PDF)

## AUTHOR INFORMATION

### Corresponding Author

\*E mail: [sspsdd@iacs.res.in](mailto:sspsdd@iacs.res.in).

### ORCID

Subhadeep Datta: 0000 0002 2611 954X

Wolfgang Wernsdorfer: 0000 0003 4602 5257

## Notes

The authors declare no competing financial interest.

## ACKNOWLEDGMENTS

The authors thank the Nanofab facility, E. Eyraud, R. Haettel, and D. Lepoittevin for technical support. S.D. acknowledges the financial support from the RTRA Nanosciences Foundation and DST SERB grant No. ECR/2017/002037. This work is partially supported by ANR PNANO project MolNanoSpin No. ANR 08 NANO 002, ERC Advanced Grant MolNanoSpin No. 226558, STEP MolSpinQIP, and the Polish National Science Centre Grant No. DEC 2017/27/B/ST3/00621. Special thanks to Romain Maurand and Józef Barnaś for fruitful discussions. Computing time at the Poznań Super computing and Networking Center is also acknowledged.

## REFERENCES

- (1) Kouwenhoven, L. P.; Marcus, C. M. *Quantum Dots*. *Phys. World* 1998, 11, 35.
- (2) Sarachik, P.; Corenzwit, E.; Longinotti, L. D. *Ab initio* Study of Spin Dependent Transport in Carbon Nanotubes with Iron and Vanadium Adatoms. *Phys. Rev. B* 2008, 78, 195405.
- (3) Goldhaber Gordon, D.; Shtrikman, H.; Mahalu, D.; Abusch Magder, D.; Meirav, U.; Kastner, M. A. Kondo Effect in a Single Electron Transistor. *Nature* 1998, 391, 156.
- (4) Kouwenhoven, L.; Glazman, L. Revival of the Kondo Effect. *Phys. World* 2001, 14, 33.
- (5) Kondo, J. Resistance Minimum in Dilute Magnetic Alloys. *Prog. Theor. Phys.* 1964, 32, 37.
- (6) Cronenwett, S.; Oosterkamp, T. J.; Kouwenhoven, L. P. A Tunable Kondo Effect in Quantum Dots. *Science* 1998, 281, 540.
- (7) Jeong, H.; Chang, A. M.; Melloch, M. R. The Kondo Effect in an Artificial Quantum Dot Molecule. *Science* 2001, 293, 2221.
- (8) Chen, J. C.; Chang, A. M.; Melloch, M. R. Transition between Quantum States in a Parallel Coupled Double quantum Dot. *Phys. Rev. Lett.* 2004, 92, 176801.
- (9) Pasupathy, A. N.; Bialczak, R. C.; Martinek, J.; Grose, J. E.; Donek, L. A. K.; McEuen, P. L.; Ralph, D. C. The Kondo Effect in the Presence of Ferromagnetism. *Science* 2004, 306, 86.
- (10) Gaass, M.; Hüttel, A. K.; Kang, K.; Weymann, I.; von Delft, J.; Strunk, Ch. Universality of the Kondo Effect in Quantum Dots with Ferromagnetic Leads. *Phys. Rev. Lett.* 2011, 107, 176808.
- (11) Craig, N. J.; Taylor, J. M.; Lester, E. A.; Marcus, C. M.; Hanson, M. P.; Gossard, A. C. Tunable Nonlocal Spin Control in a Coupled Quantum Dot System. *Science* 2004, 304, 565.
- (12) Heersche, H. B.; de Groot, Z.; Folk, J. A.; Kouwenhoven, L. P.; van der Zant, H. S. J.; Houck, A. A.; Labaziewicz, J.; Chuang, I. L. Kondo Effect in the Presence of Magnetic Impurities. *Phys. Rev. Lett.* 2006, 96, No. 017205.
- (13) Nygard, J.; Cobden, D. H.; Lindelof, P. E. Kondo Physics in Carbon Nanotubes. *Nature* 2000, 408, 342.
- (14) Paaske, J.; Rosch, A.; Wölfle, P.; Mason, N.; Marcus, C. M.; Nygard, J. Non equilibrium Singlet Triplet Kondo Effect in Carbon Nanotubes. *Nat. Phys.* 2006, 2, 408.
- (15) Choi, M. S.; Lopez, R.; Aguado, R. SU(4) Kondo Effect in Carbon Nanotubes. *Phys. Rev. Lett.* 2005, 95, No. 067204.
- (16) Korneva, G.; Ye, H.; Gogotsi, Y.; Halverson, D.; Friedman, G.; Bradley, J. C.; Kornev, K. G. Carbon Nanotubes Loaded with Magnetic Particles. *Nano Lett.* 2005, 5, 879.
- (17) Baruselli, P. P.; Smogunov, A.; Fabrizio, M.; Tosatti, E. Kondo Effect of Magnetic Impurities in Nanotubes. *Phys. Rev. Lett.* 2012, 108, 206807.
- (18) Fang, T. F.; Sun, Q. f. Kondo Phase Transitions of Magnetic Impurities in Carbon Nanotubes. *Phys. Rev. B: Condens. Matter Mater. Phys.* 2013, 87, No. 075116.
- (19) Ncube, S.; Coleman, C.; Strydom, A.; Flahaut, E.; de Sousa, A.; Bhattacharyya, S. Kondo Effect and Enhanced Magnetic Properties in



Gadolinium Functionalized Carbon Nanotube Supramolecular Complex. *Sci. Rep.* **2018**, *8*, 8057.

(20) Flahaut, E.; Peigney, A.; Laurent, Ch.; Rousset, A. Synthesis of Single Walled Carbon Nanotube Co MgO Composite Powders and Extraction of the Nanotubes. *J. Mater. Chem.* **2000**, *10*, 249.

(21) Flahaut, E.; Bacsá, R.; Peigney, A.; Laurent, C. Gram scale CCVD Synthesis of Double Walled Carbon Nanotubes. *Chem. Commun.* **2003**, *0*, 1442.

(22) Tilmaciu, C.; Soula, B.; Galibert, A.; Lukanov, P.; Datas, L.; Gonzalez, J.; Barquin, L.; Fernandez, J.; Gonzalez Jimenez, F.; Jorge, J.; Flahaut, E. Synthesis of Superparamagnetic Iron(III) Oxide Nanowires in Double Walled Carbon Nanotubes. *Chem. Commun.* **2009**, *1*, 1.

(23) Jarillo Herrero, P.; Kong, J.; van der Zant, H. S. J.; Dekker, C.; Kouwenhoven, L. P.; Franceschi, S. D. Orbital Kondo effect in Carbon Nanotubes. *Nature* **2005**, *434*, 484.

(24) Wernsdorfer, W.; Orozco, E.; Bonet, E.; Barbara, B.; Benoit, A.; Mailly, D. Classical and Quantum Magnetisation Reversal Studied in Single Nanometer Sized Particles and Clusters using Micro SQUIDS. *Phys. B* **2000**, *280*, 264.

(25) Seneor, P.; Bernand Mantel, A.; Petroff, F. Nanospintronics: when Spintronics Meets Single Electron Physics. *J. Phys.: Condens. Matter* **2007**, *19*, 165222.

(26) Sahoo, S.; Kontos, T.; Furer, J.; Hoffman, C.; Graäber, M.; Cottet, A.; Schoönenberger, C. Electric Field Control of Spin Transport. *Nat. Phys.* **2005**, *1*, 99.

(27) Zwanenburg, F. A.; van der Mast, D. W.; Heersche, H. B.; Bakkers, E. P. A.; Kouwenhoven, L. P. Electric Field Control of Magnetoresistance in InP Nanowires with Ferromagnetic Contacts. *Nano Lett.* **2009**, *9*, 2704.

(28) Quay, C. H. L.; Cumings, J.; Gamble, S. J.; de Picciotto, R.; Kataura, H.; Goldhaber Gordon, D. Magnetic Field Dependence of the Spin 1/2 and Spin 1 Kondo Effects in a Quantum Dot. *Phys. Rev. B: Condens. Matter Mater. Phys.* **2007**, *76*, 245311.

(29) Kogan, A.; Amasha, S.; Goldhaber Gordon, D.; Granger, G.; Kastner, M. A.; Shtrikman, H. Measurements of Kondo and Spin Splitting in Single Electron Transistors. *Phys. Rev. Lett.* **2004**, *76*, 1079.

(30) Babic, B.; Kontos, T.; Schönenberger, C. Kondo Effect in Carbon Nanotubes at Half Filling. *Phys. Rev. B: Condens. Matter Mater. Phys.* **2004**, *70*, 235419.

(31) Moore, J. E.; Wen, X. G. Anomalous Magnetic Splitting of the Kondo Resonance. *Phys. Rev. Lett.* **2000**, *85*, 1722.

(32) Cobden, D. H.; Bockrath, M.; McEuen, P. L.; Rinzler, A. G.; Smalley, R. E. Spin Splitting and Even Odd Effects in Carbon Nanotubes. *Phys. Rev. Lett.* **1998**, *81*, 681.

(33) Tans, S. J.; Devoret, M. H.; Dai, H.; Thess, A.; Smalley, R. E.; Geerligs, L. J.; Decker, C. Individual Single Wall Carbon Nanotubes as Quantum Wires. *Nature* **1997**, *336*, 474.

(34) Costi, T. A.; Hewson, A. C.; Zlatic, V. Transport Coefficients of the Anderson Model via the Numerical Renormalization Group. *J. Phys.: Condens. Matter* **1994**, *6*, 2519.

(35) Meir, Y.; Wingreen, N. S. Landauer Formula for the Current through an Interacting Electron Region. *Phys. Rev. Lett.* **1992**, *68*, 2512.

(36) Legeza, Ö.; Moca, C. P.; Tóth, A. I.; Weymann, I.; Zaránd, G. Manual for the Flexible DM NRG Code. *arXiv:0809.3143v1* **2008**, *68*, 2512.

(37) Wilson, K. G. The Renormalization Group: Critical Phenomena and the Kondo Problem. *Rev. Mod. Phys.* **1975**, *47*, 773.

(38) Cleuziou, J. P.; Wernsdorfer, W.; Ondarc uhu, T.; Monthieux, M. Electrical Detection of Individual Magnetic Nanoparticles Encapsulated in Carbon Nanotubes. *ACS Nano* **2011**, *5*, 2348.

(39) Datta, S.; Marty, L.; Cleuziou, J. P.; Tilmaciu, C.; Soula, B.; Flahaut, E.; Wernsdorfer, W. Magneto Coulomb Effect in Carbon Nanotube Quantum Dots Filled with Magnetic Nanoparticles. *Phys. Rev. Lett.* **2011**, *107*, 186804.

# Supplementary Information for “Detection of Spin Reversal *via* Kondo Correlation in Hybrid Carbon Nanotube Quantum Dot”

*Subhadeep Datta*<sup>1,2</sup>, *Ireneusz Weymann*<sup>3</sup>, *Anna Płomińska*<sup>3</sup>, *Emmanuel Flahaut*<sup>4</sup>, *Laëtitia Marty*<sup>2</sup>, and *Wolfgang Wernsdorfer*<sup>2,5</sup>

<sup>1</sup> School of Physical Sciences, Indian Association for the Cultivation of Science, 2A & B Raja S. C. Mullick Road, Jadavpur, Kolkata - 700032, India

<sup>2</sup> Institut Néel, CNRS & Université Joseph Fourier, BP 166, F-38042 Grenoble Cedex 9, France

<sup>3</sup> Faculty of Physics, Adam Mickiewicz University, ul. Umultowska 85, 61-614 Poznań, Poland

<sup>4</sup> CIRIMAT, Université de Toulouse, CNRS, INPT, UPS, UMR CNRS-UPS-INP N° 5085, Université Toulouse 3 Paul Sabatier, Bât. CIRIMAT, 118, route de Narbonne, 31062 Toulouse cedex 9, France

<sup>5</sup> Physikalisches Institut and Institute of Nanotechnology, Karlsruhe Institute of Technology, Wolfgang-Gaede-Strasse 1, 76131 Karlsruhe, Germany

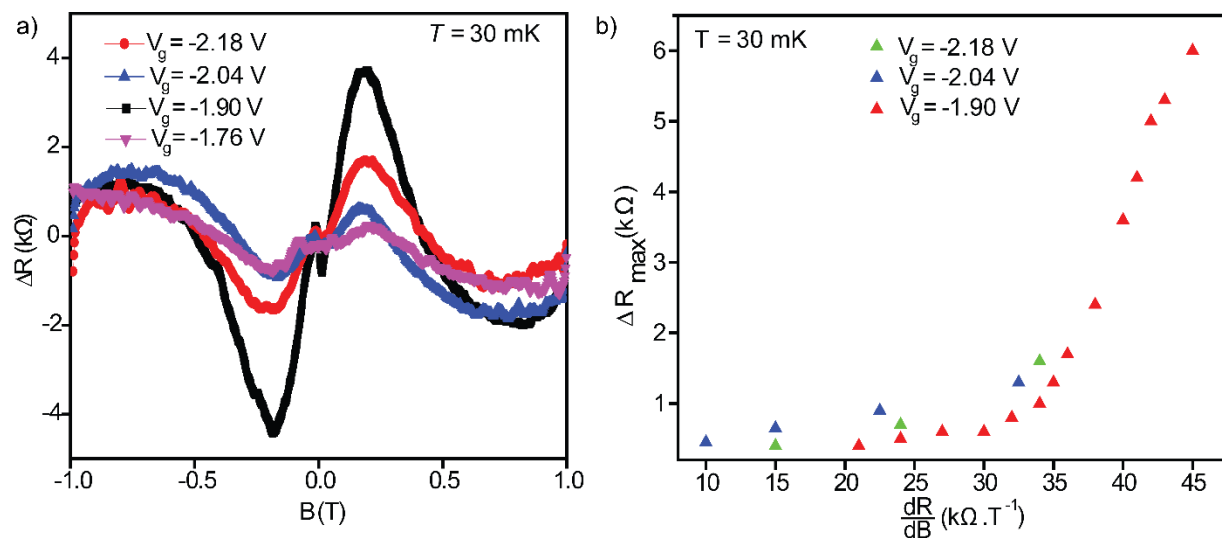
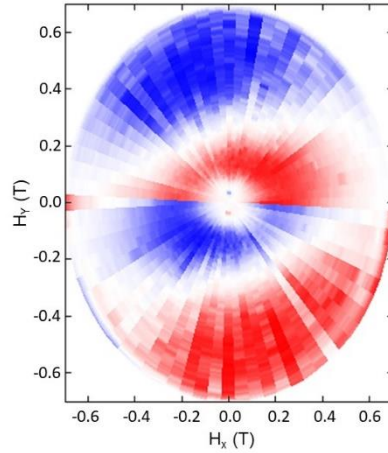


Figure S1: Hysteresis at different Kondo ridge. (a) Variation of hysteresis ( $\Delta R$ ) at different gate voltages ( $V_g = -1.76$  V,  $-1.90$  V,  $-2.04$  V and  $-2.18$  V) corresponds to deep inside the characteristic Kondo ridges at 30 mK. At  $V_g = -1.90$  V, hysteresis is maximum ( $\sim \pm 4.0$  k $\Omega$ ). (b) Slope of  $R$ - $B$  plot ( $dR/dB$ ) at different Kondo ridges. At Kondo diamond around  $V_g = -1.90$  V, the maximum hysteresis (6 k $\Omega$ ) corresponds to highest  $dR/dB$ . In other diamonds, amplitude of hysteresis is much lower than that value.



**Figure S2: Angular dependence of the switching field  $B_{sw}$  of the nanoparticles.** Magnetic field sweeps back and forth in the plane of the carbon nanotube. Hysteresis in the resistance is color plotted as a function of magnetic field in  $H_x - H_y$  plane. Hysteresis is maximum at an angle  $30^\circ$  with the x-axis.

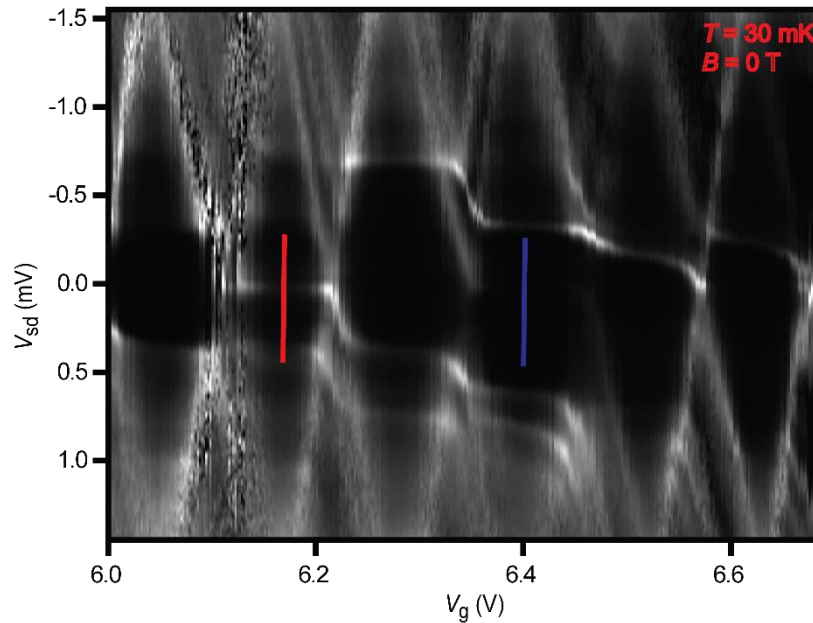




Figure S3: Coulomb diamonds of an empty carbon nanotube at  $T = 30\text{mK}$ . Regular shaped coulomb diamonds with Kondo ridges at zero bias can be clearly observed. For the bias dependent conductance data at Kondo ridges, gate voltages  $V_g = 6.17\text{ V}$ , and  $6.4\text{ V}$ , respectively (shown in vertical lines, red and blue, respectively) have been chosen in the Figure S4b.

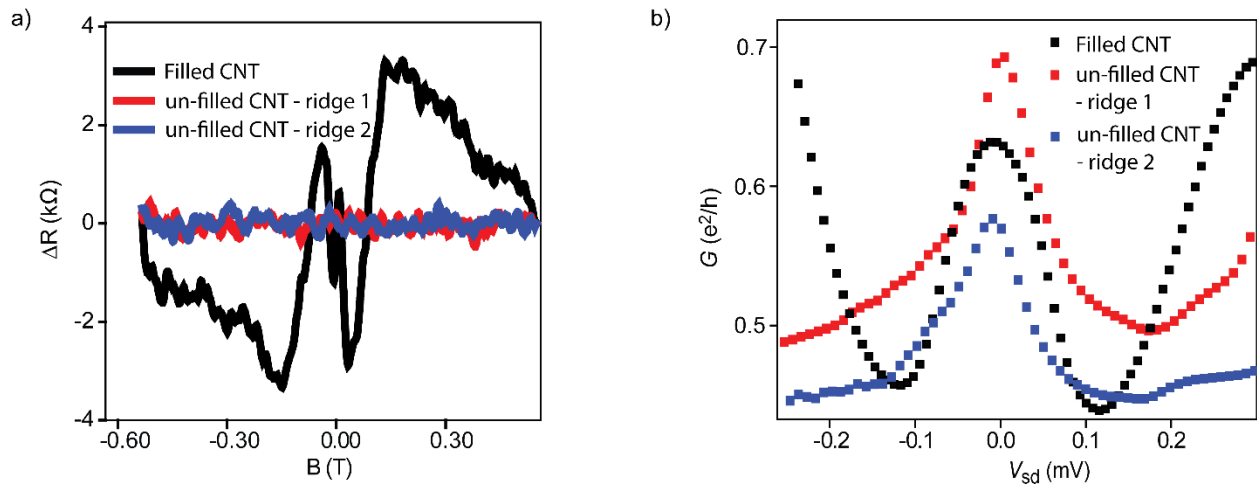


Figure S4: **Comparison of the hysteresis and zero bias conductance at Kondo ridges of un-filled and filled carbon nanotube.** a) Hysteresis of the filled CNT is much larger than that of an empty tube. b) There is no correlation between the conductance at zero bias peak (Kondo peak) and the hysteresis. Zero bias conductance of a filled tube (black dots) falls in between that of two Kondo conductance (red and blue data) of an empty tube (Figure S3).

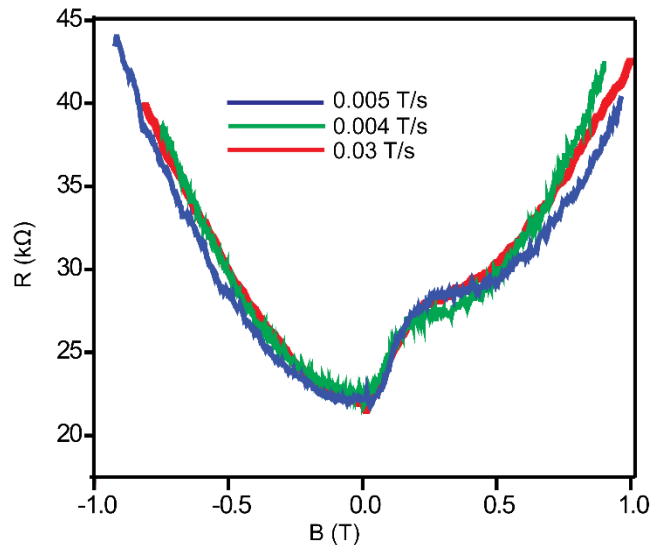


Figure S5: Magnetoresistance at different sweep rates of magnetic field. Field is swept from -1 T to +1 T. Effect of switching is similar for different sweep rates starting from 0.005 T/s to 0.03 T/s.